
FACTORIZED TENSOR NETWORKS FOR MULTI-TASK AND MULTI-DOMAIN LEARNING

Yash Garg¹, Nebiyou Yismaw¹, Rakib Hyder¹, Ashley Prater-Bennette², M. Salman Asif¹

¹ University of California Riverside, CA 92508, USA

² Air Force Research Laboratory, Rome, NY 13441, USA
ygarg002@ucr.edu, sasif@ucr.edu

ABSTRACT

Multi-task and multi-domain learning methods seek to learn multiple tasks/domains, jointly or one after another, using a single unified network. The key challenge and opportunity is to exploit shared information across tasks and domains to improve the efficiency of the unified network. The efficiency can be in terms of accuracy, storage cost, computation, or sample complexity. In this paper, we propose a factorized tensor network (FTN) that can achieve accuracy comparable to independent single-task/domain networks with a small number of additional parameters. FTN uses a frozen backbone network from a source model and incrementally adds task/domain-specific low-rank tensor factors to the shared frozen network. This approach can adapt to a large number of target domains and tasks without catastrophic forgetting. Furthermore, FTN requires a significantly smaller number of task-specific parameters compared to existing methods. We performed experiments on widely used multi-domain and multi-task datasets. We show the experiments on convolutional-based architecture with different backbones and on transformer-based architecture. We observed that FTN achieves similar accuracy as single-task/domain methods while using only a fraction of additional parameters per task.

1 Introduction

The primary objective in multi-task learning (MTL) is to train a single model to learn multiple related tasks, either jointly or sequentially. Multi-domain learning (MDL) aims to achieve the same learning objective across multiple domains. MTL and MDL techniques seek to improve overall performance by leveraging shared information across multiple tasks and domains. On the other hand, single-task or single-domain learning do not have that opportunity. Furthermore, the storage and computational cost associated with single-task/domain models quickly grows as the number of tasks/domains increases. In contrast, MTL and MDL methods can use the same network resources for multiple tasks/domains, which keeps the overall computational and storage cost small [1, 2, 3, 4, 5, 6, 7, 8, 9, 10].

In general, MTL and MDL can have different input/output configurations, but we model them as task/domain-specific network representation problems. Let us represent a network for MTL or MDL as the following general function:

$$\mathbf{y}_t = \mathbf{F}_t(\mathbf{x}) \equiv \mathbf{F}(\mathbf{x}; \mathcal{W}_t, h_t), \quad (1)$$

where \mathbf{F}_t represents a function for task/domain t that maps input \mathbf{x} to output \mathbf{y}_t . We further assume that \mathbf{F} represents a network with a fixed architecture and \mathcal{W}_t and h_t represent the parameters for task/domain-specific feature extraction and classification/inference heads, respectively. The function in (1) can represent the network for specific task/domain t using the respective \mathcal{W}_t, h_t . In the case of MTL, with T tasks, we can have T outputs $\mathbf{y}_1, \dots, \mathbf{y}_T$ for a given input \mathbf{x} . In the case of MDL, we usually have a single output for a given input, conditioned on the domain t . Our main goal is to learn the \mathcal{W}_t, h_t for all t that maximize the performance of MTL/MDL with minimal computation and memory overhead compared to single task/domain learning.

Figure 1(a),(b),(c) illustrate three typical approaches for MTL/MDL. First, we can start with a pre-trained network and fine-tune all the parameters (\mathcal{W}_t) to learn a target task/domain, as shown in Figure 1(a). Fine-Tuning approaches can transfer some knowledge from the pretrained network to the target task/domain, but they effectively use an independent

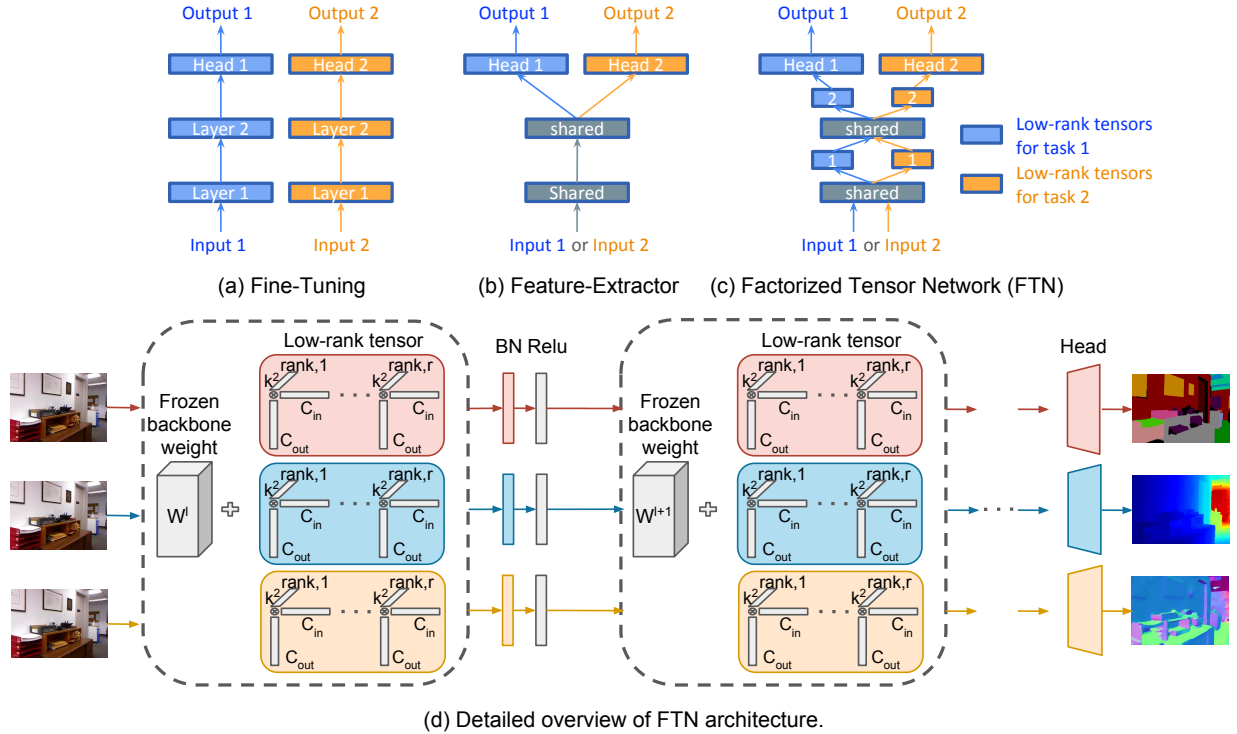


Figure 1: Overview of different MTL/MDL approaches and our proposed method. (a) Fine-Tuning trains entire network per task/domain. (b) Feature-Extractor trains a backbone network shared by all tasks/domains with task/domain-specific heads. (c) Our proposed method, Factorized Tensor Network (FTN), adapts to a new task/domain by adding low-rank factors to shared layers. (d) Detailed overview of FTN. A single network adapted to three downstream vision tasks (segmentation, depth, and surface normal estimation) by adding task-specific low-rank tensors ($\Delta\mathcal{W}_t$). Task/domain-specific blocks are shown in same colors.

network for every task/domain [1, 5, 11, 12, 13, 14]. Second, we can reduce the parameter and computation complexity by using a completely shared Feature-Extractor (i.e., $\mathcal{W}_t = \mathcal{W}_{\text{shared}}$ for all t) and learning task/domain-specific heads as last layers, as shown in Figure 1(b). While such approaches reduce the number of parameters, they often result in poor overall performance because of limited network capacity and interference among features for different tasks/domains [1, 4, 5, 15]. Third, we can divide the network into shared and task/domain-specific parameters or pathways, as shown in Figure 1(c). Such an approach can increase the network capacity, provide interference-free paths for task/domain-specific feature extraction, and enable knowledge sharing across the tasks/domains. In recent years, a number of such methods have been proposed for MTL/MDL [1, 4, 5, 9, 16, 17, 18, 19, 20, 21, 22]. While existing methods provide performance comparable to single-task/domain learning, they require a significantly large number of parameters.

In this paper, we propose a new method to divide network into shared and task/domain-specific parameters using a factorized tensor network (FTN). In particular, our method learns task/domain-specific low-rank tensor factors and normalization layers. An illustration of our proposed method is shown in Figure 1(d), where we represent network parameters as $\mathcal{W}_t = \mathcal{W}_{\text{shared}} + \Delta\mathcal{W}_t$, where $\Delta\mathcal{W}_t$ is a low-rank tensor. Furthermore, we also learn task/domain-specific normalization parameters. We demonstrate the effectiveness of our method using different MTL and MDL datasets. Our method can achieve accuracy comparable to a single-task/domain network with a small number of additional parameters. Existing parameter-efficient MTL/MDL methods [1, 2, 23] introduce small task/domain-specific parameters while others [15, 24] add many parameters to boost the performance irrespective of the task complexity. In our work, we demonstrate the flexibility of FTNs by selecting the rank according to the complexity of the task.

Contributions. The main contributions of this paper can be summarized as follows.

- We propose a new method for MTL and MDL, called factorized tensor networks (FTN), that adds task/domain-specific low-rank tensors to shared weights.
- We demonstrate that by using a fraction of additional parameters per task/domain, FTNs can achieve similar performance as the single-task/domain methods.
- Our proposed FTNs can be viewed as a plug-in module that can be added to any pretrained network and layer. We have shown this by extending FTNs to transformer-based architectures.

- We performed empirical analysis to show that the FTNs enable flexibility by allowing us to vary the rank of the task-specific tensors according to the problem complexity.

Limitations. In our experiments, we used a fixed rank for each layer. In principle, we can adaptively select the rank for different layers to further reduce the parameters. MTL/MDL models often suffer from task interference or negative transfer learning when multiple conflicting tasks are trained jointly. Our method can have similar drawbacks as we did not investigate which tasks/domains should be learned jointly. A shared backbone requires a single forward pass for all tasks while our proposed FTN would require as many forward passes as the number of tasks. Branched and tree-structures can enable different tasks to share several layers and reduce latency.

2 Related Work

Multi-task learning (MTL) methods commonly leverage shared and task-specific layers in a unified network to solve related tasks [16, 17, 18, 25, 26, 27, 28, 29, 30, 31, 32, 33]. These methods learn shared and task-specific representation through their respective modules. Optimization based methods [34, 35, 36, 37, 38] devise a principled way to evaluate gradients and losses in multi-task settings. Branched and tree-structured MTL methods [27, 39, 40] enable different tasks to share branches along a tree structure for several layers. Multiple tasks can share computations and features in any layer only if they belong to the same branch in all the preceding layers. MTL networks that incrementally learn new tasks were proposed in [9, 10]. ASTMT [10] proposed a network that emphasizes or suppresses features depending on the task at hand. RCM [9] reparameterizes the convolutional layer into non-trainable and task-specific trainable modules. We compare our proposed method with these incrementally learned networks. Adashare [8] is another related work in MTL that jointly learns multiple tasks. It learns task-specific policies and network pathways [41]. joint learning setups.

Multi-domain learning (MDL) focuses on adapting one network to multiple unseen domains or tasks. MDL setup trains models on task-specific modules built upon the frozen backbone network. This setup helps MDL networks to avoid negative transfer learning or catastrophic forgetting, which is common among multi-task learning methods. The work by [3, 6] introduces the task-specific parameters called residual adapters. The architecture introduces these adapters as a series or parallel connection on the backbone for a downstream task. Inspired by pruning techniques, Packnet [2] learns on multiple domains sequentially on a single task to decrease the overhead storage, which comes at the cost of performance. Similarly, the Piggyback [1] method uses binary masks as the module for task-specific parameters. These masks are applied to the weights of the backbone to adapt them to new domains. To extend this work, WTPB [7] uses the affine transformations of the binary mask on their backbone to extend the flexibility for better learning. BA² [4] proposed a budget-constrained MDL network that selects the feature channels in the convolutional layer. It gives parameter efficient network by dropping the feature channels based on budget but at the cost of performance. [42] paper learns the adapter modules and the plug-in architecture of the modules using NAS. Spot-Tune [24] learns a policy network, which decides whether to pass each image through Fine-Tuning or pre-trained networks. It neglects the parameter efficiency factor and emphasises more on performance. TAPS [5] adaptively learns to change a small number of layers in pre-trained network for the downstream task.

Domain adaptation and transfer learning. The work in this field usually focuses on learning a network from a given source domain to a closely related target domain. The target domains under this kind of learning typically have the same category of classes as source domains [11]. Due to this, it benefits from exploiting the labels of source domains to learn about multiple related target domains [12, 43]. Some work has a slight domain shift between source and target data like different camera views [44]. At the same time, recent papers have worked on large domain shifts like converting targets into sketch or art domains [12, 45]. Transfer learning is related to MDL or domain adaptation, but focuses on how to generalize better on target tasks [13, 14, 46]. Most of the work in this field uses the popular Imagenet as a source dataset to learn feature representation and learn to transfer to target datasets. The method proposed in [47] uses a pretrained (multi-task) teacher network and decomposes it into multiple task/knowledge-specific factor networks that are disentangled from one another. This factorization leads to sub-networks that can be fine-tuned to downstream tasks, but they rely on knowledge transfer from a teacher network that is pretrained for multiple tasks. Modular deep learning methods [48] focus on transfer learning by avoiding negative task-interference and having parameter-efficient modules.

Factorization methods in MDL/MTL. The method in [49] proposed a unified framework for MTL/MDL using semantic descriptors, but the focus is not on parameter-efficient adaptation. [50] performs MTL/MDL by factorizing each layer in the network after incorporating task-specific information along a separate dimension. Both the networks in [49] and [50] need to be retrained from scratch for new tasks/domains. In contrast, FTN can incrementally learn low-rank factors to add new tasks/domains. [51] proposed a new parameter-efficient network as a replacement for residual networks by incorporating factorized tensors. The results in [51] are limited to learning single-task networks,

where the network is only compressed by up to $\sim 60\%$. In [52], the authors proposed a network for MDL using Tucker decomposition.

Transformer-based methods in MDL/MTL There is some work in transformer-based methods. LoRA [53] is a low-rank adaptation method proposed for large language models, which freezes the pre-trained weights of the model and learns low-rank updates for each transformer layer. It updates weight matrices for query and value in every attention layer. Similarly, KAdaptation [54] proposes a parameter-efficient adaptation method for vision transformers. It represents the updates of MHSA layers using the summation of Kronecker products between shared parameters and low-rank task-specific parameters. We compared both of these methods and have shown that FTN outperforms along the number of parameters. Scaling and shifting your features (SSF) [55] is another transformer method for parameter-efficient adaptation that applies element-wise multiplication and addition to tokens after different operations. SSF in principle is similar to fine-tuning the BatchNormalization layer in convolutional layers, which has scaling and shifting trainable parameters. FTN trains the Batch Normalization layers and therefore has the same effect as scaling and shifting features when adapting to new tasks. [56] proposed inverted-pyramid multi-task transformer, performs cross-task interaction among spatial features of different tasks in a global context. The DeMT [57] proposes a deformable mixer encoder and task-aware transformer decoder. The proposed encoder leverages channel mixing and deformable convolution operation for informative features while the transformer decoder captures the task interaction.

In summary, our proposed method (FTN) offers a parameter-efficient approach to achieve performance comparable to or better than existing adaptation methods by utilizing a fraction of additional parameters. We demonstrated that, unlike other methods, easy domains do not require the transformation of the backbone by the same complex module, and we can choose the flexibility of the task/domain-specific parameter for a given task/domain.

3 Technical Details

3.1 FTN applied to Convolutional layers

In our proposed method, we use task/domain-specific low-rank tensors to adapt every convolutional layer of a pretrained backbone network to new tasks and domains. Let us assume the backbone network has L convolution layers that are shared across all task/domains. We represent the shared network weights as $\mathcal{W}_{\text{shared}} = \{\mathbf{W}_1, \dots, \mathbf{W}_L\}$ and the low-rank network updates for task/domain t as $\Delta\mathcal{W}_t = \{\Delta\mathbf{W}_{1,t}, \dots, \Delta\mathbf{W}_{L,t}\}$. To compute features for task/domain t , we update weights at every layer as $\mathcal{W}_{\text{shared}} + \Delta\mathcal{W}_t = \{\mathbf{W}_1 + \Delta\mathbf{W}_{1,t}, \dots, \mathbf{W}_L + \Delta\mathbf{W}_{L,t}\}$.

To keep our notations simple, let us only consider l th convolution layer that has $k \times k$ filters, C_{in} channels for input feature tensor, and C_{out} channels for output feature tensor. We represent the corresponding \mathbf{W}_l as a tensor of size $k^2 \times C_{in} \times C_{out}$. We represent the low-rank tensor update as a summation of R rank-1 tensors as

$$\Delta\mathbf{W}_{l,t} = \sum_{r=1}^R \mathbf{w}_{1,t}^r \otimes \mathbf{w}_{2,t}^r \otimes \mathbf{w}_{3,t}^r, \quad (2)$$

where $\mathbf{w}_{1,t}^r$, $\mathbf{w}_{2,t}^r$, $\mathbf{w}_{3,t}^r$ represent vectors of length k^2 , C_{in} , C_{out} , respectively, and \otimes represents the Kronecker product.

Apart from low-rank tensor update, we also optimize over batchnorm layers (BN) for each task/domain [58, 59]. The BN layer learns two vectors Γ and β , each of length C_{out} . The BN operation along C_{out} dimension can be defined as element-wise multiplication and addition:

$$\text{BN}_{\Gamma,\beta}(u) = \Gamma \left(\frac{u - \mathbb{E}[u]}{\sqrt{\text{Var}[u] + \epsilon}} \right) + \beta. \quad (3)$$

We represent the output of l th convolution layer for task/domain t as

$$\mathbf{Z}_{l,t} = \text{BN}_{\Gamma_t,\beta_t}(\text{conv}(\mathbf{W}_l + \Delta\mathbf{W}_{l,t}, \mathbf{Y}_{l-1,t})), \quad (4)$$

where $\mathbf{Y}_{l-1,t}$ represents the input tensor and $\mathbf{Z}_{l,t}$ represents the output tensor for l th layer. In our proposed FTN, we learn the task/domain-specific factors $\{\mathbf{w}_{1,t}^r, \mathbf{w}_{2,t}^r, \mathbf{w}_{3,t}^r\}_{r=1}^R$, and Γ_t , and β_t for every layer in the backbone network.

In the FTN method, rank R for $\Delta\mathbf{W}$ plays an important role in defining the expressivity of the adapted network. We can define a complex $\Delta\mathbf{W}$ by increasing the rank R of the low-rank tensor and taking their linear combination. Our experiments showed that this has resulted in a significant performance gain.

Initialization. In our approach, the initialization of the low-rank parameter layers and the pre-trained weights of the backbone network plays a crucial role due to their sensitivity towards performance. To establish a favorable starting

point, we adopt a strategy that minimizes substantial modifications to the frozen backbone network weights during the initialization of the task-specific parameter layers. To achieve this, we initialize each parameter layer from the xavier uniform distribution [60], thereby generating $\Delta \mathbf{W}$ values close to 0 before their addition to the frozen weights. This approach ensures the maintenance of a similar initialization state to the frozen weights at iteration 0.

To acquire an effective initialization for our backbone network, we leverage the pre-trained weights obtained from ImageNet. We aim to establish a robust and capable feature extractor for our specific task by incorporating these pre-trained weights into our backbone network.

Number of parameters. In a Fine-Tuning setup with T tasks/domains, the total number of required parameters at convolutional layer l can be calculated as $T \cdot (k^2 \times C_{in} \times C_{out})$. Whereas using our proposed FTNs, the total number of frozen backbone (\mathbf{W}_l) and low-rank R tensor ($\Delta \mathbf{W}_{l,t}$) parameters are given by $(C_{out} \times C_{in} \times k^2) + T \cdot R \cdot (C_{out} + C_{in} + k^2)$. In our results section, we have shown that the absolute number of parameters required by our method is a fraction of what the Fine-Tuning counterpart needs.

Effect of batch normalization. In our experiment section, under the ‘FC and BN only’ setup, we have shown that having task-specific batchnorm layers in the backbone network significantly affects the performance of a downstream task/domain. For all the experiments with our proposed approach, we include batch normalization layers as task-specific along with low-rank tensors and classification/decoder layer.

3.2 FTN applied to Transformers

The Vision Transformer (ViT) architecture [61] consists a series of MLP, normalization, and Multi-Head Attention (MHSA) blocks. The MHSA blocks perform n parallel attention mechanisms on sets of Key K , Query Q , and Value V matrices. Each of these matrices has dimensions of $S \times d_{model}$, where d_{model} represents the embedding dimension of the transformer, and S is the sequence length. The i -th output head (H_i) of the n parallel attention blocks is computed as

$$H_i = \text{SA}(Q\mathbf{W}_i^Q, K\mathbf{W}_i^K, V\mathbf{W}_i^V), \quad (5)$$

where $\text{SA}(\cdot)$ represents the self-attention mechanism, $\mathbf{W}_i^K, \mathbf{W}_i^Q, \mathbf{W}_i^V \in \mathbb{R}^{d_{model} \times d}$ represent the projection weights for the key, query, and value matrices, respectively, and $d = d_{model}/n$. The heads H_i are then combined using a projection matrix $\mathbf{W}_o \in \mathbb{R}^{d_{model} \times d_{model}}$ to result in the output of the MHSA block as

$$\text{MHSA}(H_1, \dots, H_n) = \text{Concat}(H_1, \dots, H_n) \cdot \mathbf{W}_o. \quad (6)$$

Following the adaptation procedure in [54], we apply our proposed factorization technique to the weights in the MHSA block. We introduce two methods for applying low-rank tensors to the attention weights:

Adapting query and value weights. Our first proposed method, *FTN (Query and Value)*, adds the low-rank tensor factors to the query \mathbf{W}^Q and value \mathbf{W}^V weights. These weights can be represented as three-dimensional tensors of size $d_{model} \times d \times n$. Using (2), we can define and learn low-rank updates $\Delta \mathbf{W}_q$ and $\Delta \mathbf{W}_v$ for the query and value weights, respectively.

Adapting output weights. Our second method, *FTN (Output projection)*, adds low-rank factors, $\Delta \mathbf{W}_o$, to the output projection weights $\mathbf{W}_o \in \mathbb{R}^{d_{model} \times d \times n}$. Similar to the previous low-rank updates, the updates to the output weights defined following (2).

Initialization. We initialize each low-rank factor by sampling from a Gaussian distribution with $\mu = 0$ and $\sigma = 0.05$. This ensures near-zero initialization, closely matching the pretrained network.

Number of parameters. The total number of parameters needed for R low-rank tensors and L MHSA blocks in FTN (Query and Value) is $2LR(d_{model} + d + n)$. FTN (Output Projection) requires only $LR(d_{model} + d + n)$ to add a similar number of factors. These additional parameters are significantly fewer than the parameters required for fully fine-tuning the four attention weights, which equals $4Ld_{model}^2$. When compared to other parameter-efficient adaptation methods such as LoRA [53] and KAdaptation [54], our methods show superior parameter efficiency. LoRA requires $4LRd_{model}$ parameters to apply low-rank factors to query and value weight matrices. KAdaptation requires $2LRd_{model} + K^3$ additional parameters for each weight, where K represents a design parameter. SSF [55] requires mLd_{model} , where m is the number of SSF modules in each transformer layer. In Table 3, we report the exact number of parameters and demonstrate that our proposed method, *FTN (Output Projection)*, has the best parameter efficiency.

4 Experiments and Results

We evaluated the performance of our proposed FTN on several MTL/MDL datasets. We conducted experiments for **1. Multi-domain classification** on convolution and transformer-based networks, and **2. Multi-task dense prediction**. For

Table 1: Number of parameters and top-1% accuracy for baseline methods, comparative methods, and FTN with varying ranks on the five domains of the ImageNet-to-Sketch benchmark experiments. Additionally, the mean top-1% of each method across all domains is shown. The ‘Params’ column gives the number of parameters used as a multiplier of those for the Feature-Extractor method, along with the absolute number of parameters required in parentheses.

Methods	Params (Abs)	Flowers	Wikiart	Sketch	Cars	CUB	mean
Fine-Tuning	$6 \times$ (141M)	95.69	78.42	81.02	91.44	83.37	85.98
Feature-Extractor	$1 \times$ (23.5M)	89.57	57.7	57.07	54.01	67.20	65.11
FC and BN only	$1.001 \times$ (23.52M)	94.39	70.62	79.15	85.20	78.68	81.60
Piggyback [1]	$6 \times [2.25 \times]$ (141M)	94.76	71.33	79.91	89.62	81.59	83.44
Packnet \rightarrow [2]	$[1.60 \times]$ (37.6M)	93	69.4	76.20	86.10	80.40	81.02
Packnet \leftarrow [2]	$[1.60 \times]$ (37.6M)	90.60	70.3	78.7	80.0	71.4	78.2
Spot-Tune [24]	$7 \times [7 \times]$ (164.5M)	96.34	75.77	80.2	92.4	84.03	85.74
WTPB [7]	$6 \times [2.25 \times]$ (141M)	96.50	74.8	80.2	91.5	82.6	85.12
BA ² [4]	$3.8 \times [1.71 \times]$ (89.3M)	95.74	72.32	79.28	92.14	81.19	84.13
TAPS [5]	$4.12 \times$ (96.82M)	96.68	76.94	80.74	89.76	82.65	85.35
FTN, R=1	$1.004 \times$ (23.95M)	94.79	73.03	78.62	86.85	80.86	82.83
FTN, R=50	$1.53 \times$ (36.02M)	96.42	78.01	80.6	90.83	82.96	85.76

each set of benchmarks, we reported the performance of FTN with different rank increments and compared the results with those from existing methods. All experiments are run on a single NVIDIA GeForce RTX 2080 Ti GPU with 12GB memory.

4.1 Multi-domain classification

4.1.1 Convolution-based networks

Datasets. We use two MTL/MDL classification-based benchmark datasets. First, ImageNet-to-Sketch [1, 2, 5, 7], which contains five different domains: Flowers [62], Cars [63], Sketch [64], Caltech-UCSD Birds (CUBs) [65], and WikiArt [66], with different classes. Second, DomainNet [67], which contains six domains: Clipart, Sketch, Painting (Paint), Quickdraw (Quick), Infograph (Info), and Real, with each domain containing an equal 345 classes. The datasets are prepared using augmentation techniques as adopted by [5].

Training details. For each benchmark, we report the performance of FTN for various choices for ranks, along with several benchmark-specific comparative and baseline methods. The backbone weights are pretrained from ImageNet, using ResNet-50 [68] for the ImageNet-to-Sketch benchmarks, and ResNet-34 on the DomainNet benchmarks to keep the same setting as [5]. On ImageNet-to-Sketch we run FTNs for ranks, $R \in \{1, 5, 10, 15, 20, 25, 50\}$ and on DomainNet dataset for ranks, $R \in \{1, 5, 10, 20, 30, 40\}$. In the supplementary material, we provide the hyperparameter details to train FTN.

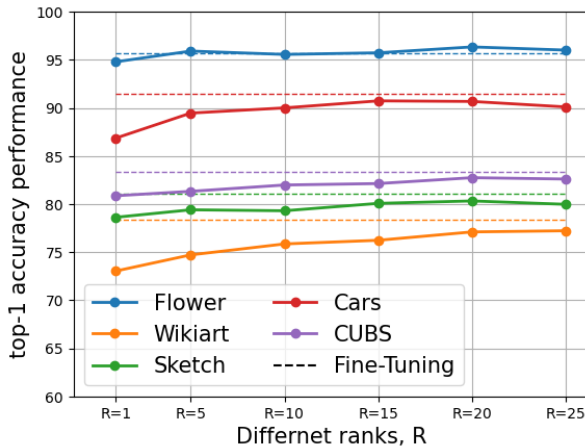
Results. We report the top-1% accuracy for each domain and the mean accuracy across all domains for each collection of benchmark experiments. We also report the number of frozen and learnable parameters in the backbone network. Table 1 compares the FTN method with other methods in terms of accuracy and number of parameters. FTN outperforms every other method while using 36.02 million parameters in the backbone with rank-50 updates for all domains. The mean accuracy performance is better than other methods and is close to Spot-Tune [24], which requires nearly 165M parameters. On the Wikiart dataset, we outperform the top-1 accuracy with other baseline methods. The performance of baseline methods is taken from TAPS [5] since we are running the experiments under the same settings.

Table 2 shows the results on the DomainNet dataset, which we compare with TAPS [5] and Adashare [8]. Again, using FTN, we significantly outperform comparison methods along the required parameters (rank-40 needs 25.22 million parameters only). Also, FTN rank-40 attains better top-1% accuracy on the Infograph and Real domain, while it attains similar performance on all other domains. On DomainNet with resnet-34 and Imagenet-to-Sketch with resnet-50 backbone, the rank-1 low-rank tensors require only 16,291 and 49,204 parameters per task, respectively. We have shown additional experiments on this dataset under a joint optimization setup in the supplementary material.

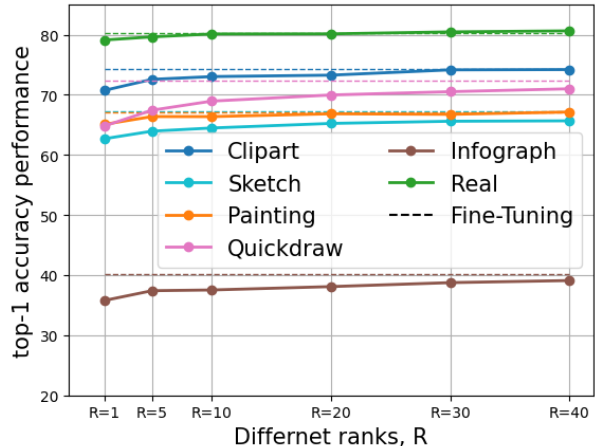
Analysis on rank. We showed the effect of rank on FTNs by performing experiments with multiple ranks on both datasets. Figure 2 shows the accuracy vs. ranks plot, where we observe a trend of performance improvement as we increase the rank from 1 to 50 on the ImageNet-to-Sketch and from 1 to 40 on the DomainNet dataset. Also, not all domains need a high rank, as Figure 2 shows that the Flowers and Cars domain attains good accuracy at rank 20 and 15, respectively. We can argue that, unlike prior works [24, 23], which consume the same task-specific module for easy and

Table 2: Performance of different methods with resnet-34 backbone on DomainNet dataset. Top-1% accuracy is shown on different domains with different methods along with the number of parameters.

Methods	Params (Abs)	Clipart	Sketch	Paint	Quick	Info	Real	mean
Fine-Tuning	$6 \times (127.68M)$	74.26	67.33	67.11	72.43	40.11	80.36	66.93
Feature-Extractor	$1 \times (21.28M)$	60.94	50.03	60.22	54.01	26.19	76.79	54.69
FC and BN only	$1.004 \times (21.35M)$	70.24	61.10	64.22	63.09	34.76	78.61	62.00
Adashare [8]	$5.73 \times (121.93M)$	74.45	64.15	65.74	68.15	34.11	79.39	64.33
TAPS [5]	$4.90 \times (104.27M)$	74.85	66.66	67.28	71.79	38.21	80.28	66.51
FTN, R=1	$1.008 \times (21.44M)$	70.73	62.69	65.08	64.81	35.78	79.12	63.03
FTN, R=40	$1.18 \times (25.22M)$	74.2	65.67	67.14	71.00	39.10	80.64	66.29



(a) Imagenet-to-sketch dataset



(b) DomainNet dataset

Figure 2: Accuracy vs Low-ranks: We show the top-1% accuracy against the different low-ranks used in our method for different domains. We start with an ‘only BN’ setup where without any low-rank we keep the BN (batchnorm) layers as task-specific. Then we show the performance improvement through our approach upon increasing the rank, R.

Table 3: We compared performance across five datasets in terms of accuracy and total parameters. FTN (O) uses low-rank factors for output projection weights, while FTN (Q&V) applies them to query and value weights. Note that the parameters mentioned exclude task-specific heads, and $5 \times (439.5M)$ denotes a fivefold increase in base network parameters, $5 \times 87.9M$.

Method	# total params	# additional params	CIFAR10	CIFAR100	DTD	STL10	FER2013	mean
Fine-tuning	$5 \times (439.5M)$	$5 \times 87.9M$	97.7	85.4	79.0	99.7	69.8	86.3
Feature extractor	$1 \times (87.9M)$	-	94.8	80.1	75.4	98.4	67.3	83.2
LoRA	$1.008 \times (88.6M)$	$5 \times 147.2K$	95.1	78.1	78.1	99.2	67.7	83.6
KAdaptation	$1.005 \times (88.3M)$	$5 \times 80.7K$	95.9	84.8	78.1	99.2	69.0	85.4
FTN (Q & V)	$1.005 \times (88.3M)$	$5 \times 81.0K$	95.8	83.4	77.1	98.7	68.5	84.7
FTN (O)	$1.002 \times (88.1M)$	$5 \times 40.5K$	96.6	84.3	76.0	98.6	69.5	85.0

complex tasks, we can provide different flexibility to each task. Also, in supplementary material, we have a heatmap plot showing the adaption of low-rank tensor at every layer upon increasing the rank.

4.1.2 Transformer-based networks

We compared our FTN method with several domain adaptation techniques for supervised image classification. Our task is to adapt a pre-trained 12-layer ViT-B-224/32 (CLIP) model obtained from [54] to new domains.

Datasets. We conducted experiments on the CIFAR10 [69], CIFAR100 [69], DTD [70], FER2013 [71], and STL10 [72] classification datasets, using the official dataset splits.

Training details. For all experiments, we set the rank to $R = 4$. We followed a similar hyper-parameter tuning procedure and implementation as outlined in [54], which utilizes grid-search to obtain the optimal learning rate for each dataset. We found that 5×10^{-6} was the optimal learning rate. Following the approach in [53], we scaled the low-rank

factors by $\frac{\alpha}{R}$, where α is a hyper-parameter, and R is the number of low-rank factors. We set $\alpha = 10$ and $\alpha = 100$ for FTN (Query and Value) and FTN (Output projection), respectively. We used a batch size of 64 and trained for 100 epochs.

Results. In Table 3, we present the classification accuracy and the total number of parameters for our proposed FTN methods, along with related model adaptation methods. Results for Fine-tuning, Feature extractor (Linear-probing), LoRA [53], and KAdaptation [54] are obtained from [54]. The first proposed method, FTN (query and value), surpasses LoRA in terms of average performance and requires fewer additional parameters. FTN (query and value) requires a comparable number of parameters to KAdaptation and performance is 0.8% lower. In contrast, FTN (output projection) requires approximately half as many additional parameters as KAdaptation but achieves comparable performance.

4.2 Multi-task dense prediction

Dataset. The widely-used NYUD dataset [73] with 795 training and 654 testing images of indoor scenes is used for dense prediction experiments in multi-task learning. The dataset contains four tasks: edge detection (Edge), semantic segmentation (SemSeg), surface normals estimation (Normals), and depth estimation (Depth). We follow the same data-augmentation technique as used by [9].

Metrics. On the tasks of the NYUD dataset, we report mean intersection over union for semantic segmentation, mean error for surface normal estimation, optimal dataset F-measure [74] for edge detection, and root mean squared error for depth estimation. We also report the number of parameters used in the backbone for each method.

Training details. ResNet-18 is used as the backbone network, and DeepLabv3+ [75] as the decoder architecture. The Fine-Tuning and Feature-Extractor experiments are implemented in the same way as in the classification-based experiments above. We showed experiments for FTNs with $R \in \{1, 10, 20, 30\}$. Further details are in the supplementary material.

Results. Table 4 shows the performance of FTN with various ranks and of other baseline comparison methods for dense prediction tasks on the NYUD dataset. We observe performance improvement by increasing flexibility through higher rank. FTN with rank-30 performs better than all comparison methods and utilizes the least number of parameters. Also, on the Depth and Edge task we can attain good performance by using only rank-20. We take the performance of baseline comparison methods from the RCM paper [9] as we run our experiments under the same setting.

Table 4: Dense prediction performance on NYUD dataset using ResNet-18 backbone with DeepLabv3+ decoder. The proposed FTN approach with $R = \{1, 10, 20, 30\}$ and other methods. The best performing method in bold.

Methods	Params (Abs)	Semseg \uparrow	Depth \downarrow	Normals \downarrow	Edge \uparrow
Single Task	$4 \times (44.68\text{M})$	35.34	0.56	22.20	73.5
Decoder only	$1 \times (11.17\text{M})$	24.84	0.71	28.56	71.3
Decoder + BN only	$1.002 \times (11.19\text{M})$	29.26	0.61	24.82	71.3
ASTMT (R-18 w/o SE) [10]	$1.25 \times (13.99\text{M})$	30.69	0.60	23.94	68.60
ASTMT (R-26 w SE) [10]	$2.00 \times (22.42\text{M})$	30.07	0.63	24.32	73.50
Series RA [3]	$1.56 \times (17.51\text{M})$	31.87	0.60	23.35	67.56
Parallel RA [6]	$1.50 \times (16.77\text{M})$	32.13	0.59	23.20	68.02
RCM [9]	$1.56 \times (17.49\text{M})$	34.20	0.57	22.41	68.44
FTN, R=1	$1.005 \times (11.23\text{M})$	29.83	0.60	23.56	72.7
FTN, R=10	$1.03 \times (11.54\text{M})$	33.66	0.57	22.15	73.5
FTN, R=20	$1.06 \times (11.89\text{M})$	34.06	0.55	21.84	73.9
FTN, R=30	$1.09 \times (12.24\text{M})$	35.46	0.56	21.78	73.8

5 Conclusion

We have proposed a simple, parameter-efficient, architecture-agnostic, and easy-to-implement FTN method that adapts to new unseen domains/tasks using low-rank task-specific tensors. In our work, we have shown FTN requires the least number of parameters compared to other baseline methods in MDL/MTL experiments and attains better or comparable performance. We can adapt the backbone network in a flexible manner by adjusting the rank according to the complexity of the domain/task. We conducted experiments with different convolutional backbones and transformer architectures for various datasets to demonstrate that FTN outperforms existing methods.

Acknowledgements

This work is supported in part by AFOSR award FA9550-21-1-0330 and ONR award N00014-19-1-2264.

References

- [1] A. Mallya, D. Davis, and S. Lazechnik, “Piggyback: Adapting a single network to multiple tasks by learning to mask weights,” in *Proceedings of the European Conference on Computer Vision (ECCV)*, 2018, pp. 67–82.
- [2] A. Mallya and S. Lazechnik, “Packnet: Adding multiple tasks to a single network by iterative pruning,” in *Proceedings of the IEEE conference on Computer Vision and Pattern Recognition*, 2018, pp. 7765–7773.
- [3] S.-A. Rebuffi, H. Bilen, and A. Vedaldi, “Learning multiple visual domains with residual adapters,” *Advances in neural information processing systems*, vol. 30, 2017.
- [4] R. Berriel, S. Lathuillere, M. Nabi, T. Klein, T. Oliveira-Santos, N. Sebe, and E. Ricci, “Budget-aware adapters for multi-domain learning,” in *Proceedings of the IEEE/CVF International Conference on Computer Vision*, 2019, pp. 382–391.
- [5] M. Wallingford, H. Li, A. Achille, A. Ravichandran, C. Fowlkes, R. Bhotika, and S. Soatto, “Task adaptive parameter sharing for multi-task learning,” in *Proceedings of the IEEE/CVF Conference on Computer Vision and Pattern Recognition*, 2022, pp. 7561–7570.
- [6] S.-A. Rebuffi, H. Bilen, and A. Vedaldi, “Efficient parametrization of multi-domain deep neural networks,” in *Proceedings of the IEEE Conference on Computer Vision and Pattern Recognition*, 2018, pp. 8119–8127.
- [7] M. Mancini, E. Ricci, B. Caputo, and S. Rota Bulò, “Adding new tasks to a single network with weight transformations using binary masks,” in *Proceedings of the European Conference on Computer Vision (ECCV) Workshops*, 2018, pp. 0–0.
- [8] X. Sun, R. Panda, R. Feris, and K. Saenko, “Adashare: Learning what to share for efficient deep multi-task learning,” *Advances in Neural Information Processing Systems*, vol. 33, pp. 8728–8740, 2020.
- [9] M. Kanakis, D. Bruggemann, S. Saha, S. Georgoulis, A. Obukhov, and L. V. Gool, “Reparameterizing convolutions for incremental multi-task learning without task interference,” in *European Conference on Computer Vision*. Springer, 2020, pp. 689–707.
- [10] K.-K. Maninis, I. Radosavovic, and I. Kokkinos, “Attentive single-tasking of multiple tasks,” in *Proceedings of the IEEE/CVF Conference on Computer Vision and Pattern Recognition*, 2019, pp. 1851–1860.
- [11] E. Tzeng, J. Hoffman, K. Saenko, and T. Darrell, “Adversarial discriminative domain adaptation,” in *Proceedings of the IEEE conference on computer vision and pattern recognition*, 2017, pp. 7167–7176.
- [12] H. Venkateswara, J. Eusebio, S. Chakraborty, and S. Panchanathan, “Deep hashing network for unsupervised domain adaptation,” in *Proceedings of the IEEE conference on computer vision and pattern recognition*, 2017, pp. 5018–5027.
- [13] B. Mustafa, A. Loh, J. Freyberg, P. MacWilliams, M. Wilson, S. M. McKinney, M. Sieniek, J. Winkens, Y. Liu, P. Bui *et al.*, “Supervised transfer learning at scale for medical imaging,” *arXiv preprint arXiv:2101.05913*, 2021.
- [14] A. Kolesnikov, L. Beyer, X. Zhai, J. Puigcerver, J. Yung, S. Gelly, and N. Houlsby, “Big transfer (bit): General visual representation learning,” in *Computer Vision—ECCV 2020: 16th European Conference, Glasgow, UK, August 23–28, 2020, Proceedings, Part V 16*. Springer, 2020, pp. 491–507.
- [15] J. O. Zhang, A. Sax, A. Zamir, L. Guibas, and J. Malik, “Side-tuning: a baseline for network adaptation via additive side networks,” in *Computer Vision—ECCV 2020: 16th European Conference, Glasgow, UK, August 23–28, 2020, Proceedings, Part III 16*. Springer, 2020, pp. 698–714.
- [16] I. Misra, A. Shrivastava, A. Gupta, and M. Hebert, “Cross-stitch networks for multi-task learning,” in *Proceedings of the IEEE conference on computer vision and pattern recognition*, 2016, pp. 3994–4003.
- [17] S. Ruder, J. Bingel, I. Augenstein, and A. Søgaard, “Latent multi-task architecture learning,” in *Proceedings of the AAAI Conference on Artificial Intelligence*, vol. 33, no. 01, 2019, pp. 4822–4829.
- [18] Y. Gao, J. Ma, M. Zhao, W. Liu, and A. L. Yuille, “Nddr-cnn: Layerwise feature fusing in multi-task cnns by neural discriminative dimensionality reduction,” in *Proceedings of the IEEE/CVF Conference on Computer Vision and Pattern Recognition*, 2019, pp. 3205–3214.
- [19] G. Strezoski, N. v. Noord, and M. Worring, “Many task learning with task routing,” in *Proceedings of the IEEE/CVF International Conference on Computer Vision*, 2019, pp. 1375–1384.

- [20] J. Liang, E. Meyerson, and R. Miikkulainen, “Evolutionary architecture search for deep multitask networks,” in *Proceedings of the genetic and evolutionary computation conference*, 2018, pp. 466–473.
- [21] Y. Gao, H. Bai, Z. Jie, J. Ma, K. Jia, and W. Liu, “Mtl-nas: Task-agnostic neural architecture search towards general-purpose multi-task learning,” in *IEEE Conference on Computer Vision and Pattern Recognition (CVPR)*, 2020.
- [22] T. Yu, S. Kumar, A. Gupta, S. Levine, K. Hausman, and C. Finn, “Gradient surgery for multi-task learning,” *Advances in Neural Information Processing Systems*, vol. 33, pp. 5824–5836, 2020.
- [23] Y. Li, N. Wang, J. Shi, J. Liu, and X. Hou, “Revisiting batch normalization for practical domain adaptation,” *arXiv preprint arXiv:1603.04779*, 2016.
- [24] Y. Guo, H. Shi, A. Kumar, K. Grauman, T. Rosing, and R. Feris, “Spottune: transfer learning through adaptive fine-tuning,” in *Proceedings of the IEEE/CVF conference on computer vision and pattern recognition*, 2019, pp. 4805–4814.
- [25] S. Liu, E. Johns, and A. J. Davison, “End-to-end multi-task learning with attention,” in *Proceedings of the IEEE/CVF conference on computer vision and pattern recognition*, 2019, pp. 1871–1880.
- [26] S. Vandenhende, S. Georgoulis, B. De Brabandere, and L. Van Gool, “Branched multi-task networks: Deciding what layers to share,” *Proceedings BMVC*, 2020.
- [27] D. Bruggemann, M. Kanakis, S. Georgoulis, and L. Van Gool, “Automated search for resource-efficient branched multi-task networks,” *Proceedings BMVC*, 2020.
- [28] D. Xu, W. Ouyang, X. Wang, and N. Sebe, “Pad-net: Multi-tasks guided prediction-and-distillation network for simultaneous depth estimation and scene parsing,” in *Proceedings of the IEEE Conference on Computer Vision and Pattern Recognition*, 2018, pp. 675–684.
- [29] Z. Zhang, Z. Cui, C. Xu, Y. Yan, N. Sebe, and J. Yang, “Pattern-affinitive propagation across depth, surface normal and semantic segmentation,” in *Proceedings of the IEEE/CVF conference on computer vision and pattern recognition*, 2019, pp. 4106–4115.
- [30] Z. Zhang, Z. Cui, C. Xu, Z. Jie, X. Li, and J. Yang, “Joint task-recursive learning for semantic segmentation and depth estimation,” in *Proceedings of the European Conference on Computer Vision (ECCV)*, 2018, pp. 235–251.
- [31] S. Vandenhende, S. Georgoulis, and L. V. Gool, “Mti-net: Multi-scale task interaction networks for multi-task learning,” in *European Conference on Computer Vision*. Springer, 2020, pp. 527–543.
- [32] L. Zhang, Q. Yang, X. Liu, and H. Guan, “Rethinking hard-parameter sharing in multi-domain learning,” in *2022 IEEE International Conference on Multimedia and Expo (ICME)*. IEEE, 2022, pp. 01–06.
- [33] L. Zhang, X. Liu, and H. Guan, “Automtl: A programming framework for automating efficient multi-task learning,” *Advances in Neural Information Processing Systems*, vol. 35, pp. 34 216–34 228, 2022.
- [34] Z. Chen, V. Badrinarayanan, C.-Y. Lee, and A. Rabinovich, “Gradnorm: Gradient normalization for adaptive loss balancing in deep multitask networks,” in *International conference on machine learning*. PMLR, 2018, pp. 794–803.
- [35] A. Kendall, Y. Gal, and R. Cipolla, “Multi-task learning using uncertainty to weigh losses for scene geometry and semantics,” in *Proceedings of the IEEE conference on computer vision and pattern recognition*, 2018, pp. 7482–7491.
- [36] M. Guo, A. Haque, D.-A. Huang, S. Yeung, and L. Fei-Fei, “Dynamic task prioritization for multitask learning,” in *Proceedings of the European conference on computer vision (ECCV)*, 2018, pp. 270–287.
- [37] X. Lin, H.-L. Zhen, Z. Li, Q.-F. Zhang, and S. Kwong, “Pareto multi-task learning,” *Advances in neural information processing systems*, vol. 32, 2019.
- [38] Z. Chen, J. Ngiam, Y. Huang, T. Luong, H. Kretschmar, Y. Chai, and D. Anguelov, “Just pick a sign: Optimizing deep multitask models with gradient sign dropout,” *Advances in Neural Information Processing Systems*, vol. 33, pp. 2039–2050, 2020.
- [39] P. Guo, C.-Y. Lee, and D. Ulbricht, “Learning to branch for multi-task learning,” in *International Conference on Machine Learning*. PMLR, 2020, pp. 3854–3863.
- [40] L. Zhang, X. Liu, and H. Guan, “A tree-structured multi-task model recommender,” in *International Conference on Automated Machine Learning*. PMLR, 2022, pp. 10–1.
- [41] E. Jang, S. Gu, and B. Poole, “Categorical reparameterization with gumbel-softmax,” in *International Conference on Learning Representations*, 2017.

- [42] H. Zhao, H. Zeng, X. Qin, Y. Fu, H. Wang, B. Omar, and X. Li, “What and where: Learn to plug adapters via nas for multidomain learning,” *IEEE Transactions on Neural Networks and Learning Systems*, vol. 33, no. 11, pp. 6532–6544, 2021.
- [43] K. Li, C. Liu, H. Zhao, Y. Zhang, and Y. Fu, “Ecacl: A holistic framework for semi-supervised domain adaptation,” in *Proceedings of the IEEE/CVF International Conference on Computer Vision*, 2021, pp. 8578–8587.
- [44] K. Saenko, B. Kulis, M. Fritz, and T. Darrell, “Adapting visual category models to new domains,” in *European Conference on Computer Vision (ECCV)*. Springer, 2010, pp. 213–226.
- [45] Y. Zhao, H. Ali, and R. Vidal, “Stretching domain adaptation: How far is too far?” *arXiv preprint arXiv:1712.02286*, 2017.
- [46] A. Dosovitskiy, L. Beyer, A. Kolesnikov, D. Weissenborn, X. Zhai, T. Unterthiner, M. Dehghani, M. Minderer, G. Heigold, S. Gelly, J. Uszkoreit, and N. Houlsby, “An image is worth 16x16 words: Transformers for image recognition at scale,” *International Conference on Learning Representations*, 2021.
- [47] X. Yang, J. Ye, and X. Wang, “Factorizing knowledge in neural networks,” in *European Conference on Computer Vision*. Springer, 2022, pp. 73–91.
- [48] J. Pfeiffer, S. Ruder, I. Vulić, and E. M. Ponti, “Modular deep learning,” *arXiv preprint arXiv:2302.11529*, 2023.
- [49] Y. Yang and T. Hospedales, “A unified perspective on multi-domain and multi-task learning,” in *3rd International Conference on Learning Representations*, 2015.
- [50] —, “Deep multi-task representation learning: A tensor factorisation approach,” in *5th International Conference on Learning Representations*, 2017.
- [51] Y. Chen, X. Jin, B. Kang, J. Feng, and S. Yan, “Sharing residual units through collective tensor factorization to improve deep neural networks,” in *IJCAI*, 2018, pp. 635–641.
- [52] A. Bulat, J. Kossaifi, G. Tzimiropoulos, and M. Pantic, “Incremental multi-domain learning with network latent tensor factorization,” in *Proceedings of the AAAI Conference on Artificial Intelligence*, vol. 34, no. 07, 2020, pp. 10470–10477.
- [53] E. J. Hu, P. Wallis, Z. Allen-Zhu, Y. Li, S. Wang, L. Wang, W. Chen *et al.*, “Lora: Low-rank adaptation of large language models,” in *International Conference on Learning Representations*, 2021.
- [54] X. He, C. Li, P. Zhang, J. Yang, and X. E. Wang, “Parameter-efficient model adaptation for vision transformers,” in *Proceedings of the AAAI Conference on Artificial Intelligence*, vol. 37, no. 1, 2023, pp. 817–825.
- [55] D. Lian, D. Zhou, J. Feng, and X. Wang, “Scaling & shifting your features: A new baseline for efficient model tuning,” *Advances in Neural Information Processing Systems*, vol. 35, pp. 109–123, 2022.
- [56] H. Ye and D. Xu, “Inverted pyramid multi-task transformer for dense scene understanding,” in *European Conference on Computer Vision*. Springer, 2022, pp. 514–530.
- [57] Y. Xu, Y. Yang, and L. Zhang, “Demt: Deformable mixer transformer for multi-task learning of dense prediction,” in *Proceedings of the AAAI conference on artificial intelligence*, vol. 37, no. 3, 2023, pp. 3072–3080.
- [58] S. Ioffe and C. Szegedy, “Batch normalization: Accelerating deep network training by reducing internal covariate shift,” in *International conference on machine learning*. pmlr, 2015, pp. 448–456.
- [59] Q. Pham, C. Liu, and H. Steven, “Continual normalization: Rethinking batch normalization for online continual learning,” in *International Conference on Learning Representations*, 2022.
- [60] X. Glorot and Y. Bengio, “Understanding the difficulty of training deep feedforward neural networks,” in *Proceedings of the thirteenth international conference on artificial intelligence and statistics*. JMLR Workshop and Conference Proceedings, 2010, pp. 249–256.
- [61] A. Dosovitskiy, L. Beyer, A. Kolesnikov, D. Weissenborn, X. Zhai, T. Unterthiner, M. Dehghani, M. Minderer, G. Heigold, S. Gelly *et al.*, “An image is worth 16x16 words: Transformers for image recognition at scale,” in *International Conference on Learning Representations*, 2020.
- [62] M.-E. Nilsback and A. Zisserman, “Automated flower classification over a large number of classes,” in *2008 Sixth Indian Conference on Computer Vision, Graphics & Image Processing*. IEEE, 2008, pp. 722–729.
- [63] J. Krause, M. Stark, J. Deng, and L. Fei-Fei, “3d object representations for fine-grained categorization,” in *Proceedings of the IEEE international conference on computer vision workshops*, 2013, pp. 554–561.
- [64] M. Eitz, J. Hays, and M. Alexa, “How do humans sketch objects?” *ACM Transactions on graphics (TOG)*, vol. 31, no. 4, pp. 1–10, 2012.
- [65] C. Wah, S. Branson, P. Welinder, P. Perona, and S. Belongie, “The caltech-ucsd birds-200-2011 dataset,” 2011.

- [66] B. Saleh and A. Elgammal, "Large-scale classification of fine-art paintings: Learning the right metric on the right feature," *International Journal for Digital Art History*, no. 2, 2016.
- [67] X. Peng, Q. Bai, X. Xia, Z. Huang, K. Saenko, and B. Wang, "Moment matching for multi-source domain adaptation," in *Proceedings of the IEEE/CVF international conference on computer vision*, 2019, pp. 1406–1415.
- [68] K. He, X. Zhang, S. Ren, and J. Sun, "Deep residual learning for image recognition," in *Proceedings of the IEEE conference on computer vision and pattern recognition*, 2016, pp. 770–778.
- [69] A. Krizhevsky, G. Hinton *et al.*, "Learning multiple layers of features from tiny images," 2009.
- [70] M. Cimpoi, S. Maji, I. Kokkinos, S. Mohamed, and A. Vedaldi, "Describing textures in the wild," in *Proceedings of the IEEE conference on computer vision and pattern recognition*, 2014, pp. 3606–3613.
- [71] I. J. Goodfellow, D. Erhan, P. L. Carrier, A. Courville, M. Mirza, B. Hamner, W. Cukierski, Y. Tang, D. Thaler, D.-H. Lee *et al.*, "Challenges in representation learning: A report on three machine learning contests," in *Neural Information Processing: 20th International Conference, ICONIP 2013, Daegu, Korea, November 3-7, 2013. Proceedings, Part III 20*. Springer, 2013, pp. 117–124.
- [72] A. Coates, A. Ng, and H. Lee, "An analysis of single-layer networks in unsupervised feature learning," in *Proceedings of the fourteenth international conference on artificial intelligence and statistics. JMLR Workshop and Conference Proceedings*, 2011, pp. 215–223.
- [73] N. Silberman, D. Hoiem, P. Kohli, and R. Fergus, "Indoor segmentation and support inference from rgbd images." *ECCV (5)*, vol. 7576, pp. 746–760, 2012.
- [74] D. R. Martin, C. C. Fowlkes, and J. Malik, "Learning to detect natural image boundaries using local brightness, color, and texture cues," *IEEE transactions on pattern analysis and machine intelligence*, vol. 26, no. 5, pp. 530–549, 2004.
- [75] L.-C. Chen, Y. Zhu, G. Papandreou, F. Schroff, and H. Adam, "Encoder-decoder with atrous separable convolution for semantic image segmentation," in *Proceedings of the European conference on computer vision (ECCV)*, 2018, pp. 801–818.
- [76] D. Ulyanov, A. Vedaldi, and V. Lempitsky, "Deep image prior," in *Proceedings of the IEEE conference on computer vision and pattern recognition*, 2018, pp. 9446–9454.
- [77] J.-Y. Zhu, P. Krähenbühl, E. Shechtman, and A. A. Efros, "Generative visual manipulation on the natural image manifold," in *Computer Vision—ECCV 2016: 14th European Conference, Amsterdam, The Netherlands, October 11-14, 2016, Proceedings, Part V 14*. Springer, 2016, pp. 597–613.
- [78] X. Pan, X. Zhan, B. Dai, D. Lin, C. C. Loy, and P. Luo, "Exploiting deep generative prior for versatile image restoration and manipulation," *IEEE Transactions on Pattern Analysis and Machine Intelligence*, vol. 44, no. 11, pp. 7474–7489, 2021.
- [79] P.-Y. Laffont, Z. Ren, X. Tao, C. Qian, and J. Hays, "Transient attributes for high-level understanding and editing of outdoor scenes," *ACM Transactions on Graphics (proceedings of SIGGRAPH)*, vol. 33, no. 4, 2014.
- [80] A. Brock, J. Donahue, and K. Simonyan, "Large scale gan training for high fidelity natural image synthesis," in *International Conference on Learning Representations*, 2019.

SUPPLEMENTARY MATERIAL

In this section, we present additional material and details to supplement the main paper.

A Dataset and training details

A.1 Imagenet-to-sketch dataset

The dataset contains five different domains: Flowers [62], Cars [63], Sketch [64], Caltech-UCSD Birds (CUBs) [65], and WikiArt [66] with 102, 195, 250, 196, and 200 classes, respectively. We randomly crop images from each domain to 224×224 pixels, along with normalization and random horizontal flipping. We report the baseline experiments, Fine-Tuning, Feature-Extractor, and 'FC and BN only' with 0.005 learning rate (lr) and SGD optimizer with no weight decay. We train for 30 epochs with a batch size 32 and a cosine annealing learning rate scheduler.

The experiments with our proposed FTN approach are learned through the Adam optimizer with lr 0.005 for low-rank layers and through the SGD optimizer with lr 0.008 for remaining trainable layers (task-specific batchnorm and classification layers). Again, we train them for 30 epochs with batch size 32 and cosine annealing scheduler. We showed the experiments for different low-ranks, $R \in \{1, 5, 10, 15, 20, 25, 50\}$.

We additionally compare the proposed FTN under diffnet backbone architecture, EfficientNet-B4. In Table 5 we have shown the performance for Fine-Tuning, Feature-Extractor, and FTN with for $R \in \{1, 10\}$. FTN irrespective of backbone architecture is giving performance close to Fine-Tuning.

Table 5: Performance on ImageNet-to-Sketch dataset under incremental setting using EfficientNet-B4 backbone with our FTN approach.

Method	Params (Abs)	Flowers	Wikiart	Sketch	Cars	CUB	mean
Fine-Tuning	6x(105.24M)	96.08	78.72	80.9	92.81	83.67	86.43
Feature extractor	1x(17.54M)	80.91	42.37	56.3	42.97	64.77	57.46
FTN, R=1	1.079x(18.93M)	93.28	74.07	79.77	87.93	82.82	83.57
FTN, R=10	1.474x(25.88M)	94.79	77.54	80.7	89.71	84.70	85.48

A.2 DomainNet dataset

This dataset contains six domains: Clipart, Sketch, Painting (Paint), Quickdraw (Quick), Infograph (Info), and Real, with an equal number of 345 classes/categories. We train the baseline experiments, Fine-Tuning, Feature-Extractor, and 'FC and BN only' with 0.005 lr with 0.0001 weight decay and SGD optimizer. Similar to the Imagenet-to-sketch dataset, we apply the same data augmentation techniques and train for 30 epochs with 32 batch size and a cosine annealing learning rate scheduler.

For our experiments with the FTN method, we train the low-rank tensor layers with Adam optimizer and 0.005 lr. The remaining layers were optimized using the SDG optimizer with the same 0.005 learning rate and no weight decay. We train the FTN networks for 30 epochs with the same learning rate scheduler. We showed our experiments for different low-ranks, $R \in \{1, 5, 10, 20, 30, 40\}$.

Table 6: Performance on DomainNet dataset under joint setting using resnet-34 backbone (initialized with jointly trained weights) with our FTN approach along with comparison methods.

Methods	Params (Abs)	Clipart	Sketch	Paint	Quick	Info	Real	mean
Fine-tuning	6x (127.68M)	77.43	69.25	69.21	71.61	41.50	80.74	68.29
Feature extractor	1x (21.28M)	76.67	65.2	65.26	52.97	35.05	76.08	61.87
FC and BN only	1.004x (21.35M)	77.07	68.34	68.76	69.06	40.63	79.07	67.15
Adashare	1x (21.28M)	75.88	63.96	67.90	61.17	31.52	76.90	62.88
TAPS	1.46x (31.06M)	76.98	67.81	67.91	70.18	39.30	78.91	66.84
FTN, R=1	1.008x (21.45M)	77.13	68.10	68.50	69.41	40.04	79.49	67.11

A.3 NYUD dataset

In multi-task learning, we use NYUD dataset, which consists of 795 training and 654 testing images of indoor scenes, for dense prediction experiments. It has four tasks: edge detection (Edge), semantic segmentation (SemSeg), surface normals estimation (Normals), and depth estimation (Depth). We evaluated the performance using optimal dataset F-measure (odsF) for edge detection, mean intersection over union (mIoU) for semantic segmentation, and mean error (mErr) for surface normals. At the same time, we report root mean squared error (RMSE) for depth. We perform random scaling in the range of [0.5, 2.0] and random horizontal flipping for data augmentation and resize each image to 425×560 . We train our baseline experiments, Fine-tuning, Feature Extractor, and 'FC and BN only' for 60 epochs with batch size 8 and polynomial learning rate scheduler. We learn the network using SGD optimizer and 0.005 learning rate with 0.9 momentum and 0.0001 weight decay.

In FTN we train for the same 60 epochs, batch size 8, and polynomial learning rate scheduler. We learn over low-rank layers using the Adam optimizer with a 0.01 learning rate and no weight decay. The remaining decoder and batchnorm layers are optimized using the same hyperparameters used for baseline experiments. This dataset shows experiments with different low-ranks, $R \in \{1, 10, 20, 30\}$.

A.4 Visual Decathlon Challenge dataset

We showed the performance of FTN on the visual decathlon challenge dataset. The experiments are performed on resnet-18 backbone with pre-trained weights initialized from Imagenet. In Table 7, we report the performance using FTN with rank $R=1, 20$ and comparison with Fine-Tuning and Feature-Extractor. We also report the total number of parameters used by each method. The FTN with rank, $R=20$ achieves accuracy significantly better than Feature-Extractor (and comparable to Fine-Tuning networks) while using only $\sim 6\%$ additional parameters compared to Feature-Extractor.

Table 7: Performance on Visual Decathlon Challenge dataset using resnet-18 backbone with FTN approach using $R=1,20$ along with the number of parameters.

Method	Params (Abs)	Airc.	C100	DPed	DTD	GTSR	Flwr	OGIt	SVHN	UCF	mean
Fine-tuning	10x(111.7M)	49.74	80.08	99.91	53.19	99.93	84.60	88.37	95.43	80.63	81.32
Feature extractor	1x(11.17M)	15.69	59.52	87.55	45.03	81.34	59.31	44.73	39.50	33.14	51.75
FTN, R=1	1.005x(11.23M)	31.29	77.38	99.36	48.98	99.83	65.98	85.12	93.06	55.94	72.99
FTN, R=20	1.06x(11.89M)	42.93	77.41	99.82	52.97	99.94	76.96	86.12	94.6	65.52	77.36

B Effect on performance with different number of low-rank factors.

We performed an experiment by removing the low-rank factors from our trained FTN backbone network at different thresholds. We perform this experiment on five domains of the Imagenet-to-sketch dataset and compute the ℓ_2 -norm of $\Delta \mathbf{W}$ at every layer. We selected equally spaced threshold values from the minimum and maximum ℓ_2 -norm and removed the low-rank factors below the threshold. The performance vs. the number of parameters of low-rank layers for different thresholds is shown in Figure 3. We observe a drop in performance on every domain as we increase the threshold and reduce the number of layers from the backbone. Interestingly, when we reduce the number of layers from 52 to 28 on the Flowers and CUBS dataset, we did not see a significant drop in accuracy.

C Visualization of changes in FTN with low-rank factors

We present the norm of low-rank factors at every adapted layer in the backbone of our FTN as a heatmap in Figures 4–5. The colors indicate relative norms because we normalized them for every network in the range 0 to 1 to highlight the relative differences. Figure 4 presents results on five domains of the Imagenet-to-sketch dataset (resnet-50 backbone), adapting every layer with rank-50 FTN. We observe the maximum changes in the last layer of the backbone network instead of the initial layers. We also show a similar trend on the DomainNet dataset with resnet-34 backbone where maximum changes occur in the network’s later layer (see Figure 6). We observe from Figure 5 that on the wikiart domain of the Imagenet-to-sketch dataset, the layers in the backbone network become more adaptive upon increasing the rank of FTN. The rank-50 FTN has more task adaptive layers than the rank-1 FTN on the wikiart domain.

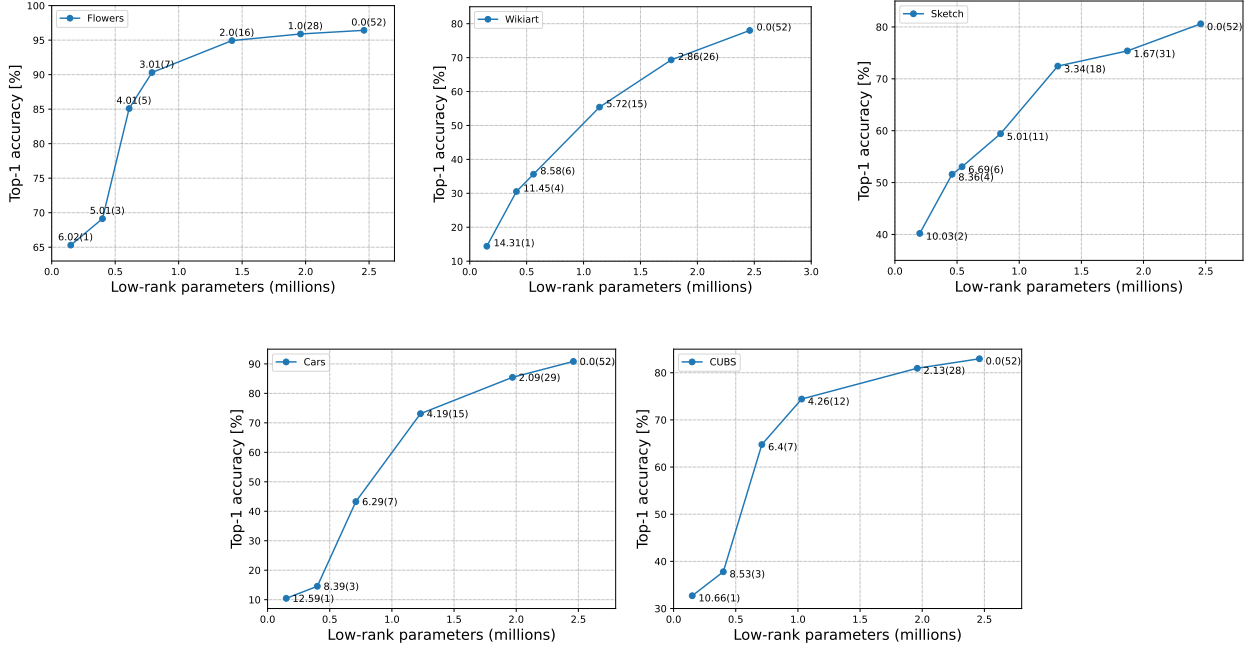


Figure 3: Performance on five domains of the Imagenet-to-sketch dataset as we remove the low-rank parameters. We selected the number of layers in the backbone based on a moving threshold. We annotate the specified threshold at each marker point and the number of affected layers (in parentheses).

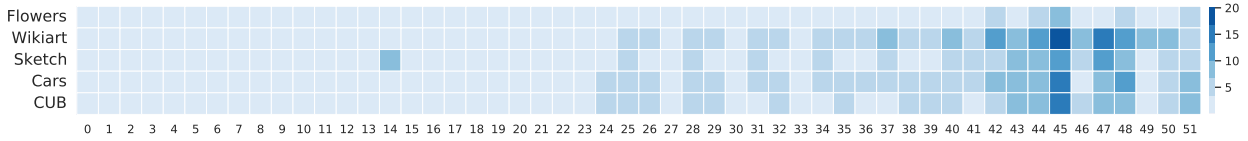


Figure 4: Norm of low-rank factors in the adapted backbone layers for different domains of the Imagenet-to-sketch dataset with $R = 50$.

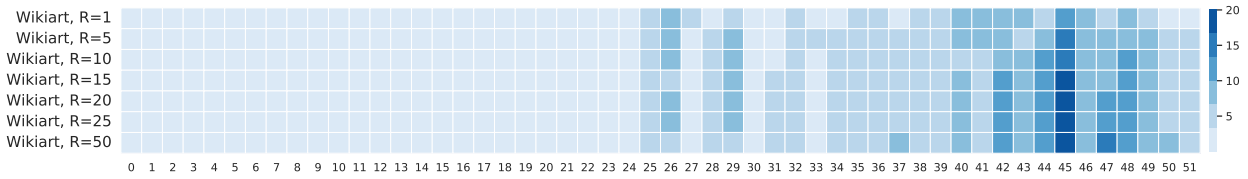


Figure 5: Norm of low-rank factors in the adapted backbone layers for different values of $R \in \{1, 5, 10, 15, 20, 25, 50\}$ with the wikiart domain of the Imagenet-to-sketch dataset.

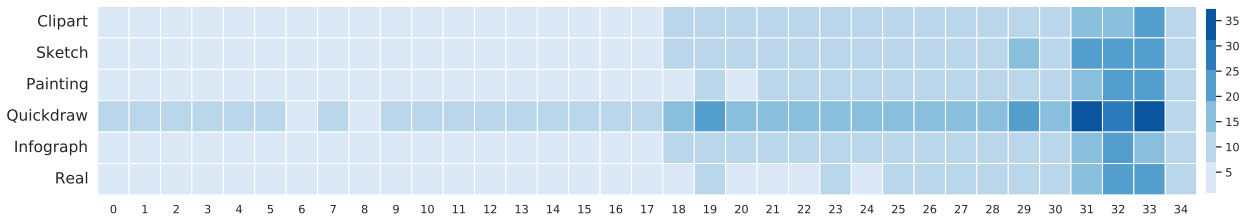


Figure 6: Norm of low-rank factors in the adapted backbone layers for different domains of the DomainNet dataset with $R = 40$.

D Results on DomainNet dataset under joint setting

We performed additional experiments under a joint learning setup on the DomainNet dataset. A single model is trained jointly on all the domains of the dataset with Fine-Tuning setup. Table 6 summarizes the results for the performance of the DomainNet dataset under a joint setup. The domains under this setting share information among each other for all parameters. The Fine-Tuning experiment achieves the overall best performance, but at the expense of a large number of parameters. We observe poor performance for the shared Feature Extractor, since that does not learn any additional task-specific parameters. The results in the third row show that by changing just the task-specific batchnorm layers in the jointly trained backbone, we can achieve better results than TAPS and Adashare. Our FTN with just $R = 1$ also outperforms Adashare and TAPS.

E Analysis on ΔW_t in FTN vs post-training factorization

We have done experimental results to show that FTN learns explicit low-rank representation instead of a module that stores low-rank tensors. For post-training factorization, we consider $\Delta W_t = W_t - W$, i.e. computing the difference between the weights of the fine-tuned network (W_t) and the original network (W). We have compressed or performed low-rank approximation on the trained ΔW_t using CP, Tensor train (TT), and SVD matrix factorization. We performed experiments on ImageNet-to-Sketch dataset with resnet-50 and efficient-net backbone with $R \in \{1, 10, 20, 30, 40, 50\}$. Table 8 depicts that low-rank approximation of trained ΔW_t causes severe performance degradation. For instance, $R=1$, average accuracy for ImageNet-to-Sketch with resnet-50 drops to nearly 27%. As R increases, the accuracy improves for all the factorization approaches, but they remain lower than FTN results. From Table 10 the difference between FTN and post-training factorization is even more striking in the case of Efficient-Net. For instance, $R=1$, average accuracy drops to nearly 5%. As R increases, the number of parameters increases sharply but even with 2x more parameters, the average accuracy of post-training low-rank factorization remains lower than FTN with $R=1$. The Table 9, 11 depicts the approximation error (averaged over all the layers) for different values R and every task. We report average error and standard deviation over the layers for a subset of R . We observe that as R increases approximation error reduces, which leads to improvement in accuracy. Nevertheless, approximation error remains significant even with large R , which is the reason why accuracy remains significantly less than fine-tuned weights. In all cases, accuracy for tasks depends on approximation error (Flowers and CUBS do better than Wikiart and Sketch because the approximation error is small).

Table 8: Low-rank factorization of weight increments on ImageNet-to-Sketch dataset with resnet-50 backbone.

Method	Params (Abs)	Flowers	Wikiart	Sketch	Cars	CUB	mean
Fine-Tuning(arbitrary $\Delta W_t = W_t - W$)	6x(141M)	95.69	78.42	81.02	91.44	83.32	85.98
FTN, R=1	1.004x(23.95M)	94.79	73.03	78.62	86.85	80.86	82.83
FTN, R=50	1.53x(36.02M)	96.42	78.01	80.6	90.83	82.96	85.76
ΔW with R=1 (CP)	1.009x(23.71M)	64.73	5.36	6.6	10.17	51.97	27.76
ΔW with R=10 (CP)	1.09x(25.67M)	88.58	10.97	48.02	56.42	70.59	54.91
ΔW with R=20 (CP)	1.185x(27.84M)	92.76	20.83	61.88	78.65	76.98	66.22
ΔW with R=30 (CP)	1.27x(30.02M)	94.15	37.68	71.27	83.56	79.81	73.29
ΔW with R=40 (CP)	1.37x(32.197)	94.6	46.33	74.73	86.74	81.2	76.72
ΔW with R=50 (CP)	1.46x(34.37M)	94.75	56.65	77.32	87.95	82.03	79.74
ΔW with R=1 (TT)	1.009x(23.71M)	64.55	5.38	7.38	10.32	51.78	27.88
ΔW with R=10 (TT)	1.15x(27.18M)	88.4	8.87	52.33	57.64	70.14	55.47
ΔW with R=20 (TT)	1.31x(30.86M)	92.73	22.26	62.7	78.34	77.01	66.60
ΔW with R=30 (TT)	1.46x(34.53M)	94.13	37.66	70.9	84.16	80.22	73.41
ΔW with R=40 (TT)	1.62x(38.21M)	94.68	50.13	75.05	87.12	81.34	77.66
ΔW with R=50 (TT)	1.78x(41.89M)	94.89	57.24	77.55	88.17	82.24	80.01
ΔW with R=1 (SVD)	1.01x(23.79M)	62.69	6.19	5.88	12.21	50.21	27.43
ΔW with R=10 (SVD)	1.12x(26.42M)	88.75	12.3	52.00	54.21	71.26	55.70
ΔW with R=20 (SVD)	1.24x(29.34M)	92.81	20.89	63.35	77.63	77.03	66.34
ΔW with R=30 (SVD)	1.37x(32.26M)	94.18	35.2	69.77	83.65	79.48	72.45
ΔW with R=40 (SVD)	1.49x(35.18M)	94.55	51.04	74.38	86.64	80.96	77.51
ΔW with R=50 (SVD)	1.62x(38.13M)	94.89	58.92	76.45	87.82	81.71	79.95

Table 9: Average (std deviation) approximation error for low-rank factorization of weight increments ΔW on ImageNet-to-Sketch dataset with resnet-50 backbone.

Method	Flowers	Wikiart	Sketch	Cars	CUB	mean
ΔW norm	0.88 (1.18)	31.15 (34.21)	10.89 (11.95)	2.23 (2.97)	1.66 (2.54)	9.36 (10.57)
ΔW with R=1 (CP)	0.85 (1.15)	30.56 (34.18)	10.64 (11.93)	2.16 (2.92)	1.60 (2.50)	9.16 (10.53)
ΔW with R=10 (CP)	0.63 (0.87)	26.53 (31.00)	9.07 (10.71)	1.72 (2.33)	1.27 (2.00)	7.84 (9.38)
ΔW with R=20 (CP)	0.49 (0.66)	23.14 (28.01)	7.81 (9.55)	1.40 (1.87)	1.03 (1.58)	6.77 (8.33)
ΔW with R=30 (CP)	0.40 (0.52)	20.38 (25.42)	6.81 (8.55)	1.17 (1.85)	0.85 (1.29)	5.922 (7.52)
ΔW with R=40 (CP)	0.33 (0.43)	18.11 (23.19)	6.00 (7.72)	1.003 (1.32)	0.73 (1.08)	5.23 (6.74)
ΔW with R=50 (CP)	0.27 (0.36)	16.20 (21.29)	5.34 (7.02)	0.87 (1.16)	0.63 (0.93)	4.66 (6.15)
ΔW with R=1 (TT)	0.85 (1.15)	30.59 (34.20)	10.66 (11.94)	2.16 (2.92)	1.60 (2.50)	9.17 (10.54)
ΔW with R=10 (TT)	0.62 (0.87)	25.90 (30.72)	8.84 (10.57)	1.68 (2.31)	1.24 (1.99)	7.65 (9.29)
ΔW with R=20 (TT)	0.48 (0.66)	22.11 (27.42)	7.45 (9.28)	1.33 (1.83)	0.98 (1.56)	6.47 (8.15)
ΔW with R=30 (TT)	0.38 (0.52)	19.08 (24.53)	6.37 (8.19)	1.09 (1.49)	0.80 (1.26)	5.54 (7.19)
ΔW with R=40 (TT)	0.30 (0.42)	16.58 (22.00)	5.50 (7.26)	0.91 (1.25)	0.66 (1.04)	4.79 (6.39)
ΔW with R=50 (TT)	0.25 (0.34)	14.50 (19.81)	4.78 (6.47)	0.77 (1.07)	0.56 (0.88)	4.17 (5.71)
ΔW with R=1 (SVD)	0.85 (1.15)	30.57 (34.21)	10.65 (11.93)	2.16 (2.92)	1.61 (2.50)	9.16 (10.54)
ΔW with R=10 (SVD)	0.65 (0.88)	26.55 (31.23)	9.11 (10.78)	1.74 (2.36)	1.29 (2.02)	7.86 (9.45)
ΔW with R=20 (SVD)	0.51 (0.69)	23.13 (28.36)	7.86 (9.67)	1.43 (1.92)	1.05 (1.61)	6.79 (8.45)
ΔW with R=30 (SVD)	0.42 (0.56)	20.34 (25.84)	6.87 (8.72)	1.20 (1.61)	0.88 (1.33)	5.94 (7.61)
ΔW with R=40 (SVD)	0.34 (0.46)	18.01 (23.63)	6.06 (7.90)	1.03 (1.38)	0.75 (1.13)	5.23 (6.9)
ΔW with R=50 (SVD)	0.29 (0.39)	16.05 (21.69)	5.38 (7.21)	0.89 (1.22)	0.65 (0.98)	4.65 (6.29)

Table 10: Low-rank factorization of weight increments on ImageNet-to-Sketch dataset with efficient-net backbone.

Method	Params (Abs)	Flowers	Wikiart	Sketch	Cars	CUB	mean
Fine-Tuning (arbitrary $\Delta W_t = W_t - W$)	6x(105.24M)	96.08	78.72	80.9	92.81	83.67	86.43
FTN, R=1	1.079x(18.93M)	93.28	74.07	79.77	87.93	82.82	83.57
FTN, R=10	1.474x(25.88M)	94.79	77.54	80.7	89.71	84.70	85.48
ΔW with R=1 (CP)	1.04x(18.31M)	20.08	0.65	0.4	0.83	3.02	4.99
ΔW with R=10 (CP)	1.43x(25.24M)	76.83	0.65	10.5	21.68	49.43	31.81
ΔW with R=20 (CP)	1.87x(32.95M)	91.72	0.65	46.63	72.73	73.23	56.99
ΔW with R=30 (CP)	2.31x(40.66M)	94.68	2.32	68.53	85.59	79.27	65.07
ΔW with R=40 (CP)	2.75x(48.37M)	95.35	26.45	63.52	89.65	81.79	71.35
ΔW with R=50 (CP)	2.79x(49.02M)	95.45	41.42	76.5	91.03	82.34	77.34
ΔW with R=1 (TT)	1.04x(18.31M)	20.00	0.65	0.4	0.8	3.52	5.07
ΔW with R=10 (TT)	1.43x(25.2M)	77.02	0.65	11.17	22.62	49.19	32.13
ΔW with R=20 (TT)	1.84x(32.3M)	91.49	0.66	47.5	72.94	72.51	57.02
ΔW with R=30 (TT)	2.20x(38.76M)	94.78	2.37	68.38	86.08	79.46	66.21
ΔW with R=40 (TT)	2.52x(44.3M)	95.32	31.64	74.6	89.79	81.95	74.66
ΔW with R=50 (TT)	2.80x(49.22M)	95.63	63.18	78.5	91.07	82.84	82.24
ΔW with R=1 (SVD)	1.07x(18.77M)	23.74	0.65	0.4	1.02	6.02	6.366
ΔW with R=10 (SVD)	1.51x(26.59M)	76.84	0.65	11.33	22.81	49.43	32.21
ΔW with R=20 (SVD)	1.86x(32.68M)	91.59	0.66	47.62	72.96	72.52	57.07
ΔW with R=30 (SVD)	2.20x(38.63M)	94.78	2.37	68.38	86.08	79.46	66.21
ΔW with R=40 (SVD)	2.51x(44.14M)	95.32	31.64	74.6	89.75	81.95	74.65
ΔW with R=50 (SVD)	2.79x(49.09M)	95.63	63.18	78.5	91.07	82.84	82.24

Table 11: Average (std deviation) approximation error for low-rank factorization of weight increments ΔW on ImageNet-to-Sketch dataset with efficient-net backbone.

Method	Flowers	Wikiart	Sketch	Cars	CUB	mean
ΔW norm	0.88 (1.18)	31.15 (34.21)	10.89 (11.95)	2.23 (2.97)	1.66 (2.54)	9.36 (10.57)
ΔW with R=1 (CP)	0.85 (1.15)	30.56 (34.18)	10.64 (11.93)	2.16 (2.92)	1.60 (2.50)	9.16 (10.53)
ΔW with R=10 (CP)	0.63 (0.87)	26.53 (31.00)	9.07 (10.71)	1.72 (2.33)	1.27 (2.00)	7.84 (9.38)
ΔW with R=20 (CP)	0.49 (0.66)	23.14 (28.01)	7.81 (9.55)	1.40 (1.87)	1.03 (1.58)	6.77 (8.33)
ΔW with R=30 (CP)	0.40 (0.52)	20.38 (25.42)	6.81 (8.55)	1.17 (1.85)	0.85 (1.29)	5.922 (7.52)
ΔW with R=40 (CP)	0.33 (0.43)	18.11 (23.19)	6.00 (7.72)	1.003 (1.32)	0.73 (1.08)	5.23 (6.74)
ΔW with R=50 (CP)	0.27 (0.36)	16.20 (21.29)	5.34 (7.02)	0.87 (1.16)	0.63 (0.93)	4.66 (6.15)
ΔW with R=1 (TT)	0.85 (1.15)	30.59 (34.20)	10.66 (11.94)	2.16 (2.92)	1.60 (2.50)	9.17 (10.54)
ΔW with R=10 (TT)	0.62 (0.87)	25.90 (30.72)	8.84 (10.57)	1.68 (2.31)	1.24 (1.99)	7.65 (9.29)
ΔW with R=20 (TT)	0.48 (0.66)	22.11 (27.42)	7.45 (9.28)	1.33 (1.83)	0.98 (1.56)	6.47 (8.15)
ΔW with R=30 (TT)	0.38 (0.52)	19.08 (24.53)	6.37 (8.19)	1.09 (1.49)	0.80 (1.26)	5.54 (7.19)
ΔW with R=40 (TT)	0.30 (0.42)	16.58 (22.00)	5.50 (7.26)	0.91 (1.25)	0.66 (1.04)	4.79 (6.39)
ΔW with R=50 (TT)	0.25 (0.34)	14.50 (19.81)	4.78 (6.47)	0.77 (1.07)	0.56 (0.88)	4.17 (5.71)
ΔW with R=1 (SVD)	0.85 (1.15)	30.57 (34.21)	10.65 (11.93)	2.16 (2.92)	1.61 (2.50)	9.16 (10.54)
ΔW with R=10 (SVD)	0.65 (0.88)	26.55 (31.23)	9.11 (10.78)	1.74 (2.36)	1.29 (2.02)	7.86 (9.45)
ΔW with R=20 (SVD)	0.51 (0.69)	23.13 (28.36)	7.86 (9.67)	1.43 (1.92)	1.05 (1.61)	6.79 (8.45)
ΔW with R=30 (SVD)	0.42 (0.56)	20.34 (25.84)	6.87 (8.72)	1.20 (1.61)	0.88 (1.33)	5.94 (7.61)
ΔW with R=40 (SVD)	0.34 (0.46)	18.01 (23.63)	6.06 (7.90)	1.03 (1.38)	0.75 (1.13)	5.23 (6.9)
ΔW with R=50 (SVD)	0.29 (0.39)	16.05 (21.69)	5.38 (7.21)	0.89 (1.22)	0.65 (0.98)	4.65 (6.29)

F Multi-domain image generation

A deep generative network \mathbf{G} , parameterized by \mathcal{W} , can learn to map a low-dimensional latent code \mathbf{z} to a high-dimensional natural image \mathbf{x} [76, 77, 78]. To find a latent representation for a set of images given a pre-trained generative network, we can solve the following optimization problem:

$$\min_{z_i} \sum_{i=1}^N \|x_i - \mathbf{G}(z_i; \mathcal{W})\|_p^p. \quad (7)$$

The work in [78] as well as our experimental results show that this approach is very limited in handling complex and diverse images. If \mathbf{x} is an image that belongs to a domain that is different from the source domain used to train the generator, we are not guaranteed to find a latent vector \mathbf{z}^* such that $\mathbf{x} \approx \mathbf{G}(\mathbf{z}^*)$. We showed FTNs can be used to expand the range of \mathbf{G} by reparametrizing it as $\mathbf{G}(z_i; \mathcal{W}, \Delta\mathcal{W}_t)$, where $\Delta\mathcal{W}_t$ are the domain-specific low-rank factors and Batch Normalization parameters. By optimizing over the latent vectors z_i and domain specific parameters, we learned to generate images from new domains.

Dataset. We used the multi-domain Transient Attributes [79] dataset. The dataset contains a total of 8571 images with 40 annotated attribute labels. Each label is associated with a score in the $[-1, 1]$ range. We utilize the associated confidence score for each season to build our collection of images for each season. Additionally, we only selected images that were captured during daytime. Our training set consisted of 1875 summer, 1405 spring, 1353 autumn, and 2566 winter images. We normalized each image to the range of $[-1, 1]$ and resized them to a resolution of 128×128 .

Training details. Our base network follows the BigGAN architecture [80] that was pre-trained for 100k iterations on ImageNet using 128×128 images. We trained all the networks in this experiment using Adam optimizer. We used a learning rate of 0.05 for the low-rank tensors and a learning rate of 0.001 for the linear layers. We did not use any weight decay. We trained for 2000 epochs with a cosine annealing learning rate scheduler and an early stopping criterion ranging from 200 to 600 iterations.

Results. Table 12 shows the performance, in terms of Peak Signal-to-Noise Ratio (PSNR), for three methods. Our proposed FTN network achieved a comparable performance to the single-domain networks. Each single domain network has 71.4M trainable parameters, while the FTN network adds an additional 3.9M parameters per domain over the base network. Figure 7 and 8 show examples of images generated by our proposed FTN network. In addition, table 13 shows the average performance of our FTN network under different rank settings. We observe a performance increase by increasing the rank R of our low-rank factors.

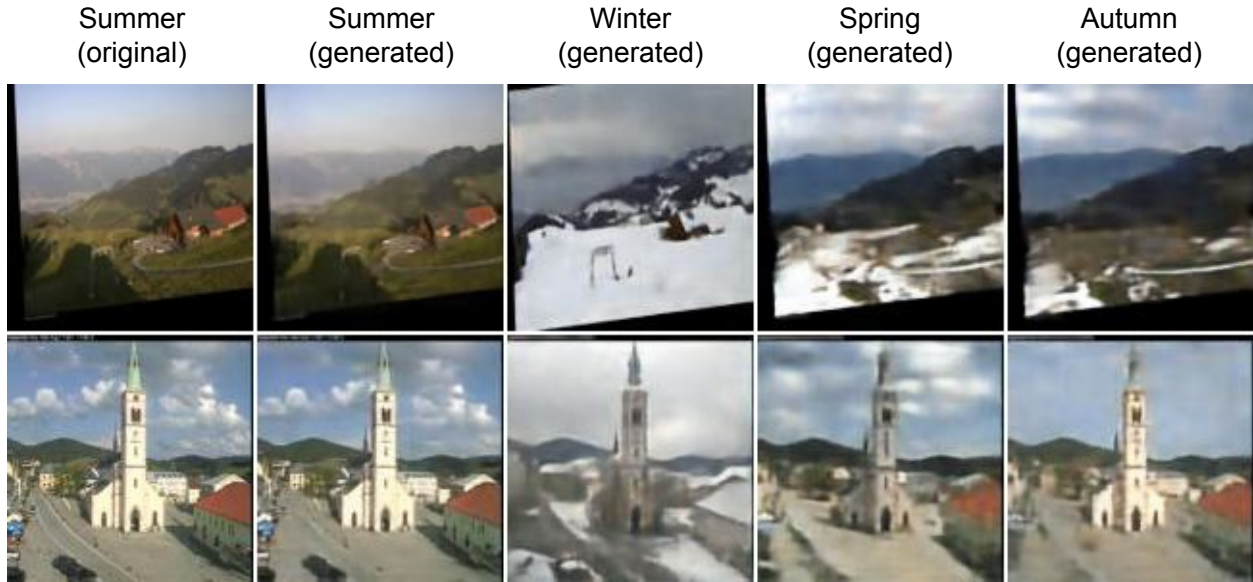


Figure 7: Generated images for different seasons using FTN.

Table 12: Image generation PSNR for different methods and seasons

Season	Single domain	FTN
Summer	25.30	25.30
Winter	21.30	22.23
Spring	22.07	20.50
Autumn	19.87	20.08

Table 13: FTN PSNR for image generation under $R = \{20, 50\}$

Season	Rank 20	Rank 50
Winter	18.11	22.23
Spring	18.89	20.50
Autumn	17.95	20.08

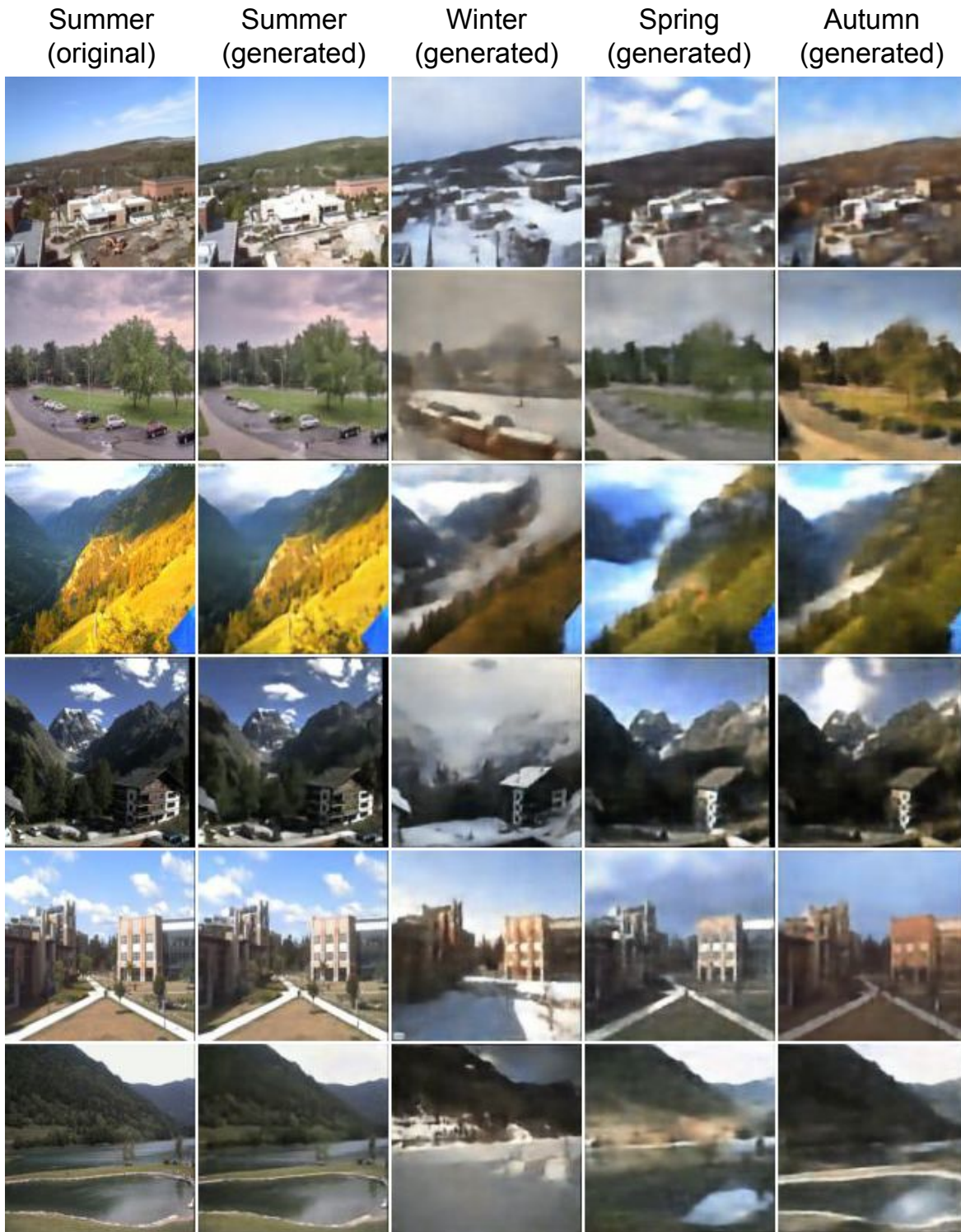


Figure 8: Additional generated images for different seasons using FTN.